Stem Cell Reports, Volume *8*

Supplemental Information

Common Telomere Changes during In Vivo Reprogramming and Early Stages of Tumorigenesis

Rosa M. Marión, Isabel López de Silanes, Lluc Mosteiro, Benjamin Gamache, María Abad, Carmen Guerra, Diego Megías, Manuel Serrano, and Maria A. Blasco

Supplemental Figures

Figure S1. NANOG expression in reprogrammed tissues. Related to Figures 1, 2, 3 and 4

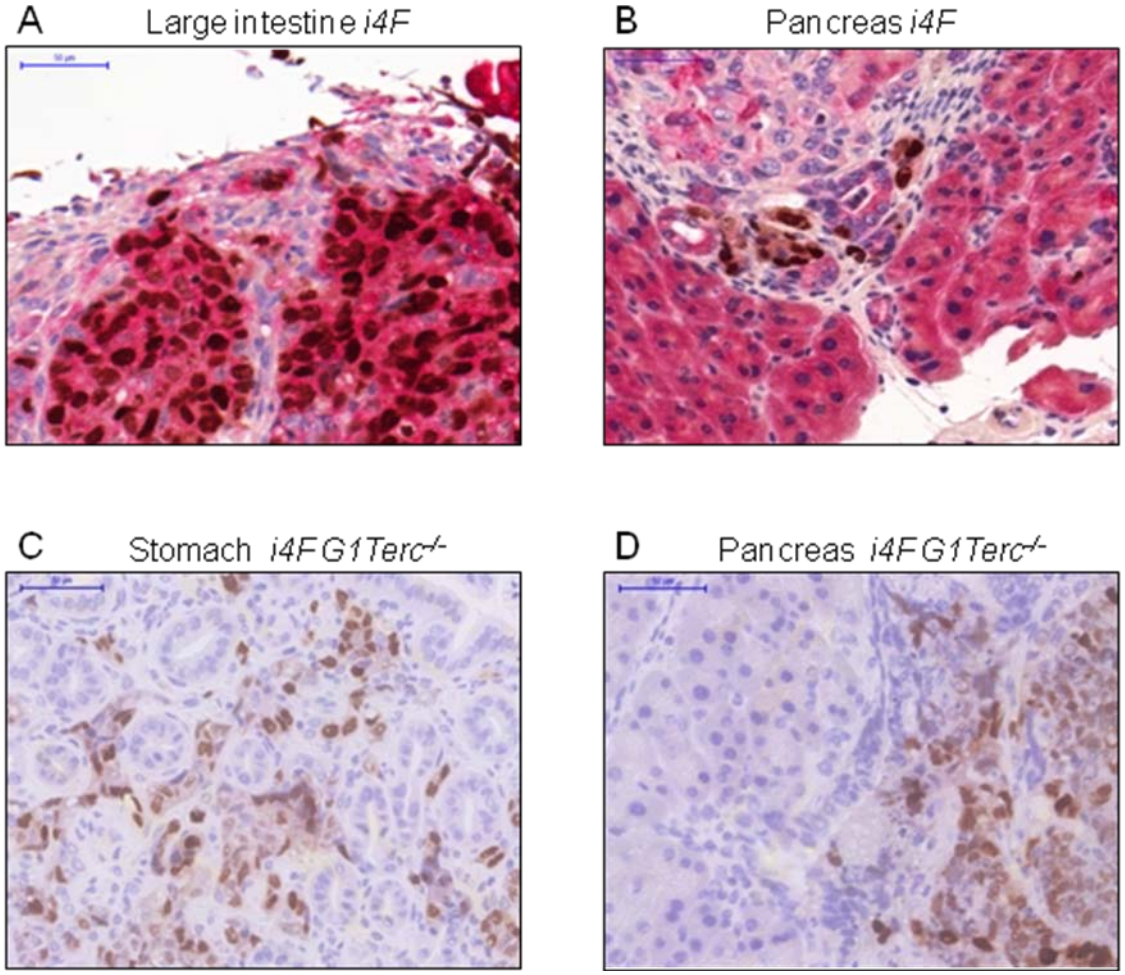

Figure S1. NANOG expression in reprogrammed tissues. Double immunohistochemistry of NANOG (dark brown) and cytokeratin 19 (CK19, magenta) in **(A)** the large intestine and **(B)** the pancreas of *i4F* reprogrammable mice. Immunohistochemistry of NANOG (dark brown) in **(C)** the stomach and **(D)** the pancreas of *i4F G1Terc*$^{-/-}$ reprogrammable mice. Scale bars 50μM.

Figure S2. TERC probe detects TERC at telomeres. Related to Figure 2

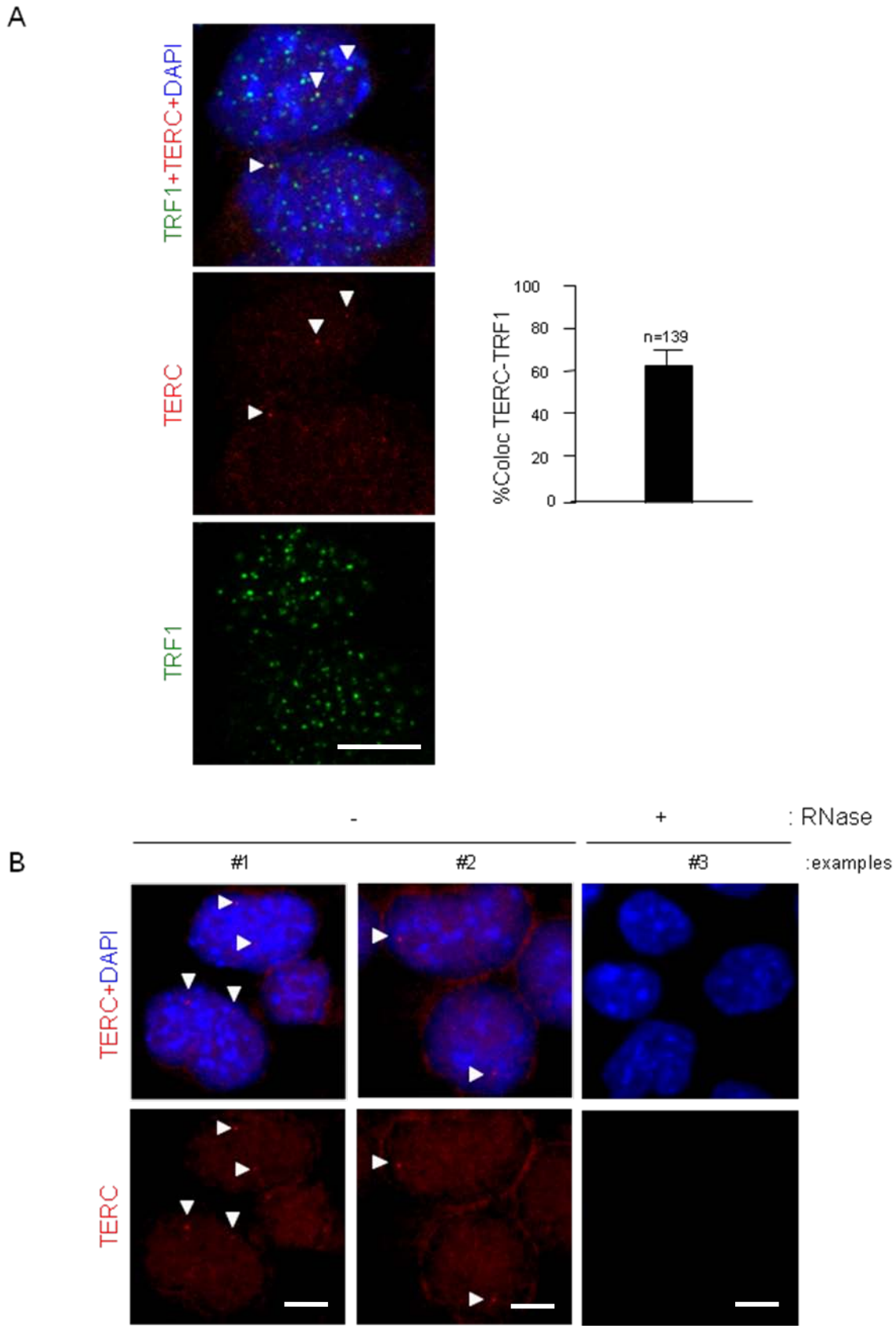

Figure S2. TERC probe detects TERC at telomeres. (A) Left, confocal images corresponding to TERC detection by RNA-FISH (red) followed by immunostaining to detect the telomeric protein TRF1 (green) in iPS cells. Arrowheads indicate the presence of co-localization (partial overlay) of TERC with TRF1. Note that colocalization of TERC foci with TRF1 confirms the specificity of the probe. Right, percentage of TERC co-localization with TRF1 per nuclei is represented. N= number of nuclei analyzed. Error bars, SE. Scale bars 10μM. **(B)** Confocal images corresponding to TERC detection by RNA-FISH (red) in iPS cells untreated or treated with RNase. Arrowheads indicate the presence of TERC spots. Scale bars 10μM.

Figure S3. TRF1 expression increases during *in vivo* reprogramming. Related to Figure 4

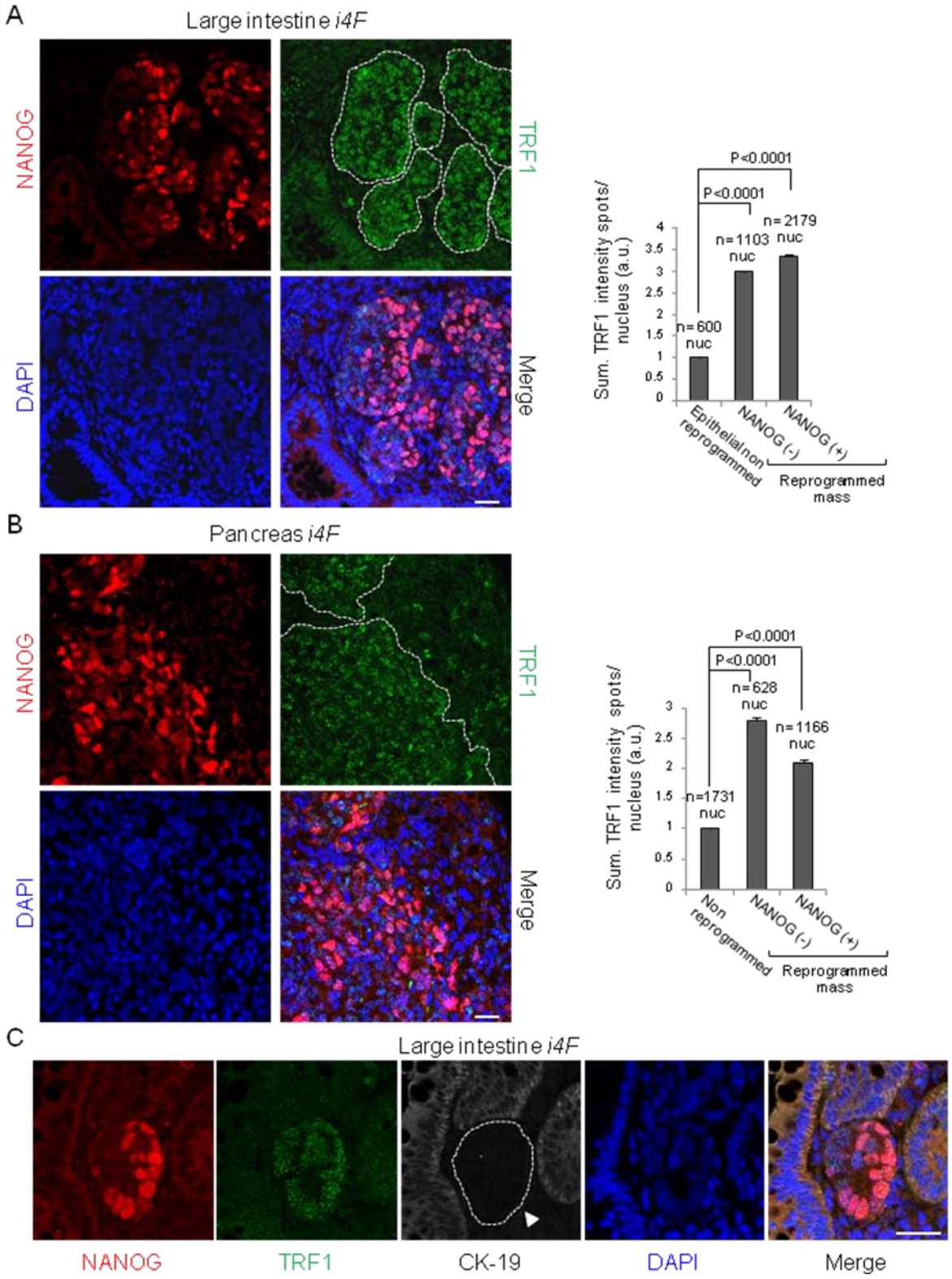

Figure S3. TRF1 expression increases during *in vivo* reprogramming. (A) Left, representative images of double immunofluorescence against NANOG (red) and TRF1 (green) proteins in the large intestine of

a reprogrammable mouse after induction of *in vivo* reprogramming. Note that TRF1 is highly expressed in the reprogrammed mass (white dotted area). Scale bars, 25μm. Right, quantification of TRF1 expression in nuclei of the cells from the reprogrammed mass and the corresponding epithelial non-reprogrammed control cells from the same tissue. Error bars, SE. Statistical analysis was performed using the Student´s t test. n, number of nuclei. Number of mice analyzed=3. (**B**) Same staining as **A** in the pancreas of a reprogrammable mouse. White dotted lines mark reprogrammed area. Scale bars, 25μm. Error bars, SE. Statistical analysis was performed using the Student´s t test. n, number of nuclei. Number of mice analyzed=3. **C**) Triple immunofluorescence against NANOG (red), TRF1 (green) and cytokeratin 19 (white) in the large intestine of a reprogrammable mouse after induction of *in vivo* reprogramming. Scale bars, 25μm. Note (white dotted area) that all the cells in the reprogrammed area, including those not expressing NANOG, have lost the expression of the epithelial marker, indicating that they have been indeed reprogrammed *in vivo*.

Figure S4. ***In vivo*** **reprogramming induces profound changes in heterochromatin conformation. Related to Figure 1**

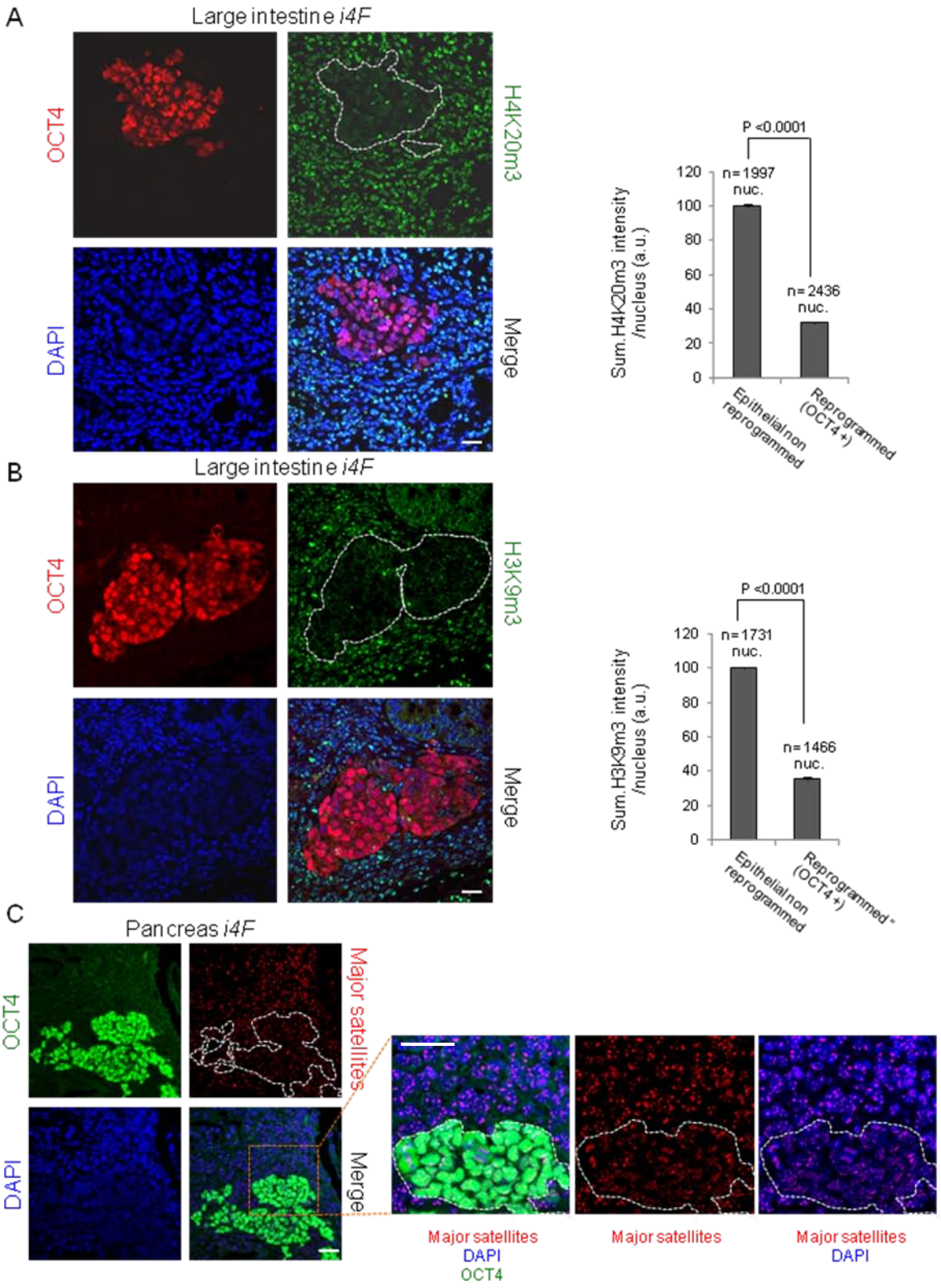

Figure S4. ***In vivo*** **reprogramming induces profound changes in heterochromatin conformation.** **(A)** Left, representative images of double immunofluorescence against OCT4 (red) and H4K20m3 (green) proteins in the large intestine of WT reprogrammable mouse after induction of *in vivo* reprogramming. White dotted lines mark reprogrammed area. Scale bars, 25μm. Right, quantification of H4K20m3 expression in nuclei of *in vivo* reprogrammed cells and the corresponding non-reprogrammed control cells. n, number of nuclei. Number of mice analyzed=3. Error bars, SE. Statistical analysis was performed using the Student´s t test. **(B)** Left, representative images of double immunofluorescence against OCT4 (red) and H3K9m3 (green) proteins in the large intestine of a WT reprogrammable mouse after induction of *in vivo* reprogramming. White dotted lines mark reprogrammed area. Scale bars, 25μm. Right, quantification of H3K9m3 expression in nuclei of *in vivo* reprogrammed cells and the corresponding non-reprogrammed control cells. A clear decrease in the expression of both heterochromatic marks can be observed in the reprogrammed cells. Error bars, SE. Statistical analysis was performed using the Student´s t test. n, number of nuclei. Number of mice analyzed=3. **(C)** Left, representative immuno-FISH images showing OCT4 (green) and major satellites (red) in the pancreas of a reprogrammable mouse after induction of *in vivo* reprogramming. White dotted lines mark reprogrammed area. Scale bars, 25μm. Right, zoomed panel of the selected area. Scale bars, 25μm. Note the drastic reorganization of pericentric heterochromatin in the *in vivo* reprogrammed cells.

Figure S5. Reduced SA1 expression in reprogrammed tissues. Related to Figure 1

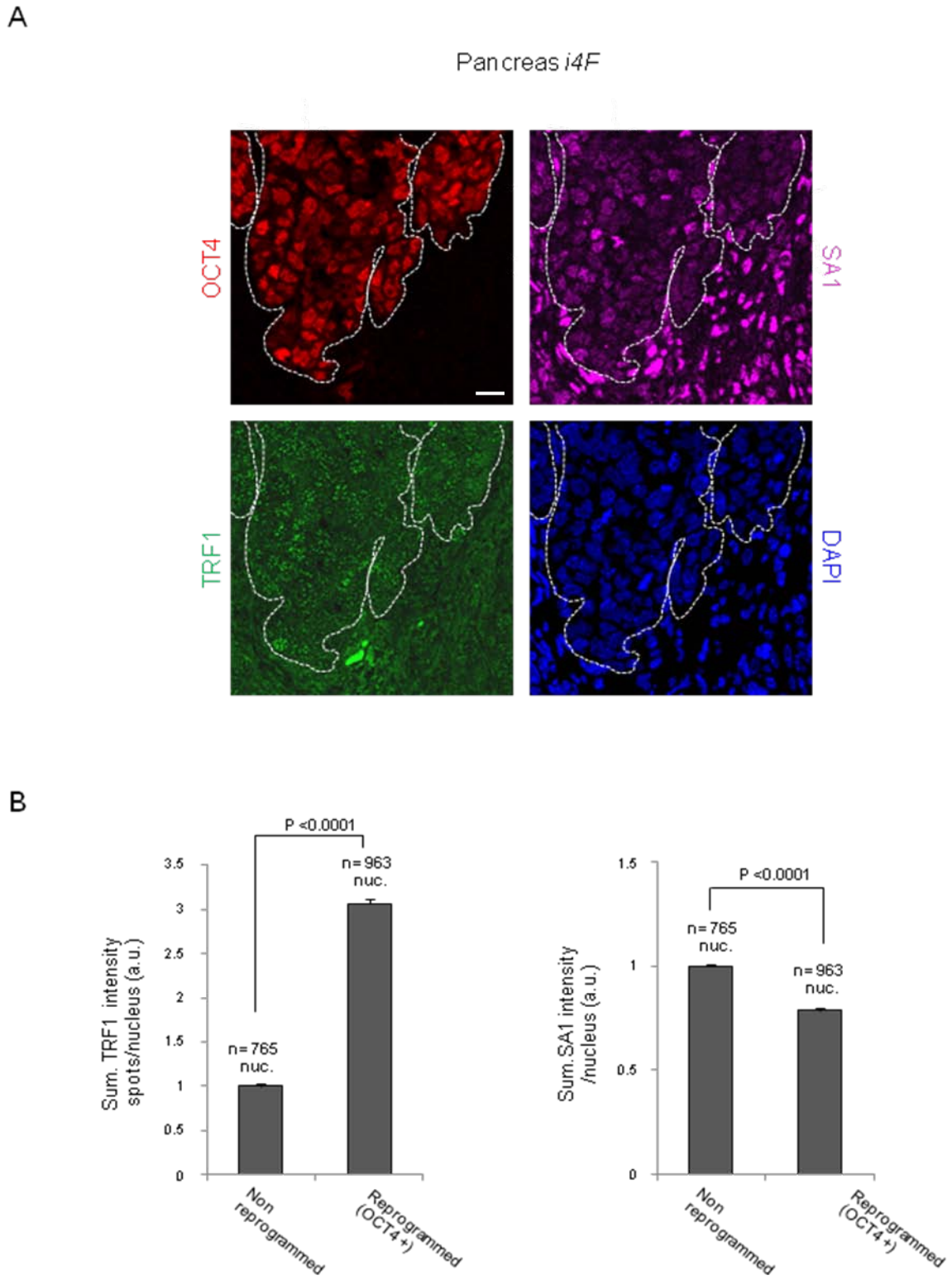

Figure S5. Reduced SA1 expression in reprogrammed tissues. (A) Representative images of triple immunofluorescence against OCT4 (red), SA1 (magenta) and TRF1 (green) proteins in the pancreas of *i4F* reprogrammable mouse after induction of *in vivo* reprogramming. White dotted lines mark reprogrammed area. A clear reduction in the expression of SA1 protein can be observed in the reprogrammed cells, corresponding with the presence of OCT4 and high TRF1 expression. **(B)** Quantification of TRF1 and SA1 expression in nuclei of *in vivo* reprogrammed cells and the corresponding non-reprogrammed control cells. Error bars, SE. Statistical analysis was performed using the Student´s t test. n, number of nuclei. Number of mice analyzed=3. Scale bars, 25μm.

Figure S6. Telomere elongation in some early pancreatic lesions of *ElasK-Ras*^{G12V} mice. Related to Figure 6

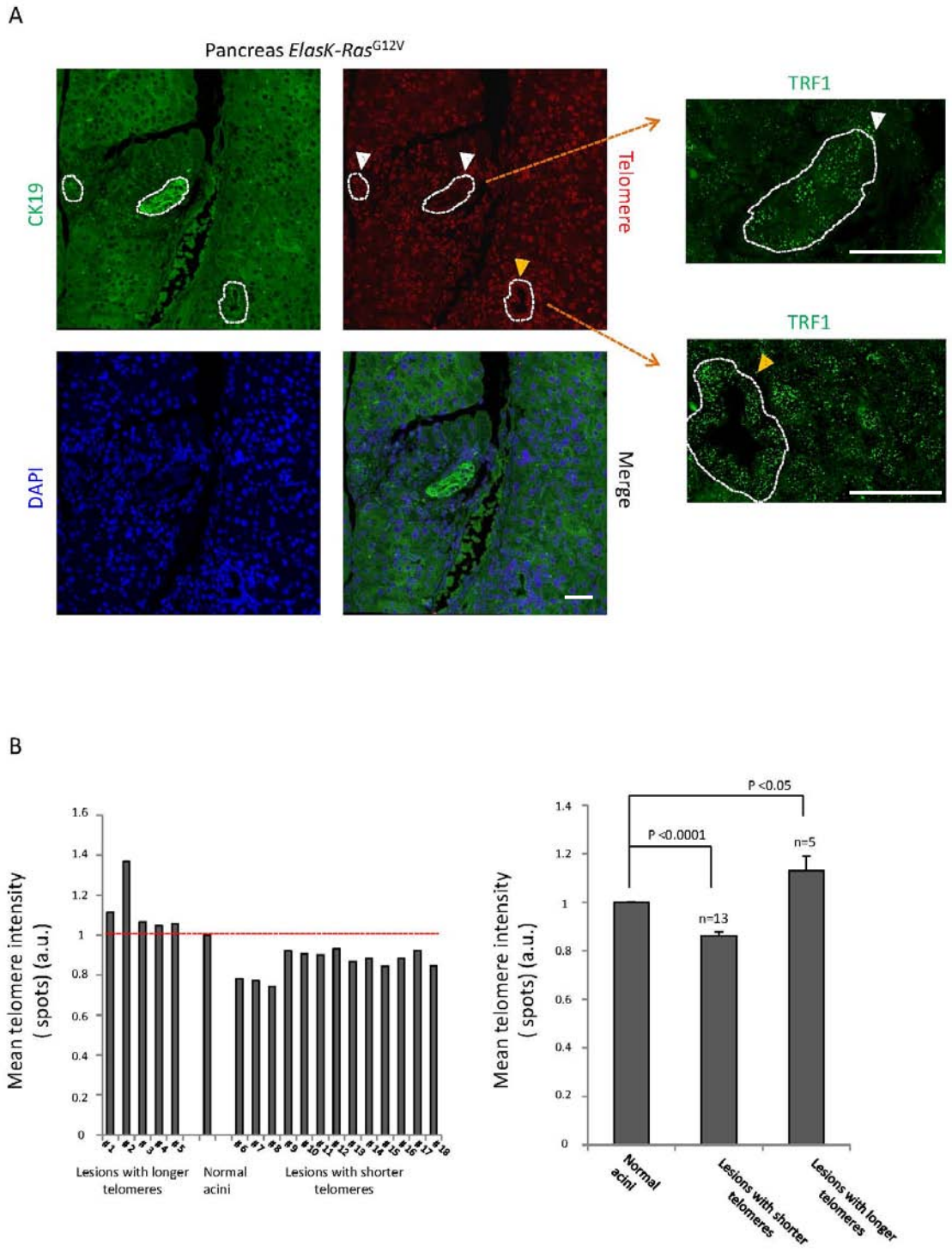

Figure S6. Telomere elongation in some early pancreatic lesions of *ElasK-Ras*^{G12V} mice. (A) Left, representative immuno-FISH images showing CK19 (green) and telomeres (red) in pancreas of *ElasK-Ras*^{G12V} mice. White dotted lines mark pancreatic lesions. A fraction of lesions show elongated telomeres when compared to normal acinar cell (yellow arrow), while other show shorter telomeres than control

cells (white arrows). Right, immunofluorescence against TRF1 in the same lesions that were analized by immuno-FISH. Note that TRF1 is increased in both lesions, independently of telomere elongation. Scale bars, 25μm. **(B)** Quantification of telomere signal in the nuclei of pancreatic lesions cells when compared to normal acinar cells from the same tissue shows that telomere length increases in 28% of the lesions analyzed. Error bars, SE. Statistical analysis was performed using the Student´s t test. n, number of pancreatic lesions analyzed. Number of mice analyzed=4.

Supplemental Experimental Procedures

Generation of *i4F Terc*$^{-/-}$ and *eGFP-TRF1*$^{+/KI}$ i4F reprogrammable mice

We generated the telomerase-deficient reprogrammable mouse line *i4F Terc*$^{-/-}$ by crossing the reprogrammable mouse line *i4F* (Abad et al., 2013) to a telomerase deficient mouse line *Terc*$^{-/-}$ (Blasco et al., 1997). Only mice from the first generation of the telomerase-deficient reprogrammable line (*i4F G1Terc*$^{-/-}$) were used in this work. The *eGFP-TRF1*$^{+/KI}$ i4F reprogrammable mice containing a hypomorphic allele of TRF1 was generated by crossing the reprogrammable mouse line *i4F* (Abad et al., 2013) to the *eGFP-TRF1*$^{+/KI}$ mouse line (Schneider et al., 2013). All mice were generated and maintained at the Spanish National Cancer Center under specific pathogen-free conditions in accordance with the recommendation of the Federation of European Laboratory Animal Science Associations.

Histopathology and Immunohistochemistry

Tissue samples were fixed in 10% formaline, paraffine-embedded and cut in 2.5 µm sections, which were mounted in superfrostplus portaobjects and re-hydrated. For histopathological analysis, sections were stained with hematoxylin and eosin (H&E). For immunohistochemistry, paraffine sections underwent antigenic exposure process. The following primary antibodies were used: for NANOG, Cell Signalling Technology, 8822; for cytokeratin 19 (CK19), CNIO Monoclonal Antibodies Core Unit, AM-TROMA III. Slides were then incubated with the corresponding secondary antibodies conjugated with peroxidase from Dako.

Isolation of *in vivo* iPS cells from reprogrammed pancreas

Reprogrammed pancreas from induced *i4F* mice were washed in PBS and chopped in iPS cell medium (standard ES medium supplemented with knockout serum replacement, KSR, Invitrogen). Dissociated tissues were filtered through a 40 µm cell strainer and cultured on feeder fibroblasts, with daily medium changes. Colonies of iPS cells became visible at the microscope and were picked and expanded on feeder fibroblasts using standard procedures.

RNA isolation and qRT-PCR analysis

Pancreas were homogenized in guanidine thiocyanate (GTG) using a rotor-stator homogenizer. Total RNA was isolated from pancreas or iPS cells using traditional phenol:chloroform extraction, and then was treated with DNase to remove genomic DNA contamination. Total RNA (1µg) was reverse transcribed using the iScript cDNA Synthesis Kit (BIO-RAD 170-8891) according to the manufacturer's instructions. Quantitative polymerase chain reaction (qRT-PCR) reactions were set up in triplicate. *Terc, TRF1 and OCT4* expression was normalized to *ACTB* expression The primers used for qRT-PCR were as follows: ACTB Forward, 5´-GGCACCACACCTTCTACAATG-3´, ACTB Reverse, 5´-GTGGTGGTGAAGCTGTAG-3´, TERC Forward, 5´-TCATTAGCTGTGGGTTCTGGT-3´, TERC Reverse, 5´-TGGAGCTCCTGCGCTGACGTT-3´, OCT4 Forward, 5´-TCTTTCCACCAGGCCCCCGGCTC-3´, OCT4 Reverse, 5´-TGCGGGCGGACATGGGGAGATCC-3´, TRF1 Forward, 5´-TCTAAGGATAGGCCAGATGCCA-3´, TRF1 Reverse, 5´-CTGAAATCTGATGGAGCACGT-3´.

RNA-FISH combined with immunostaining

Tissues embedded in OCT were cryosectioned at 12µm. Sections were washed in PBS and placed in cytobuffer (100 mM NaCl/300 mM sucrose/3 mM $MgCl_2$/10 mM Pipes, pH 6.8) for 30 sec, washed in cytobuffer with 0.5% Triton X-100 for 30 sec, washed in cytobuffer for 30 sec, and then fixed for 10 min in 4% PFA in PBS. Sections were then dehydrated in 70%, 80%, 95%, and 100% ethanol, air-dried, and hybridized overnight at 45°C with TERC RNA probe in hybridization buffer [2×sodium saline citrate (SSC)/50% formamide]. Slides were washed two times for 15 min in hybridization buffer at 48°C, 10 min in 2×SSC at 48°C, 10 min in 1×SSC at 48ºC, 5 min in 4xSSC at room temperature, 5 min in 4×SSC containing 0.1% Tween20, and 5 min in 4×SSC at room temperature. After fixation in 4% PFA in PBS, sections were blocked for 1-hour at 37ºC in PBS containing 5% (w/v) BSA and permeabilized with cold Triton 0.1% in PBS for 20 min. Antibodies against OCT4 (Abcam ab19857) were incubated on the slides in blocking solution for 60 min at 37ºC. The slides were washed three times in PBST, overlaid with goat anti-rabbit IgG–Alexa 488 (ThermoFisher Scientific A11008) for 1 h in blocking solution at 37°C, washed three times in PBST and mounted in Prolong with DAPI (Life Technologies). Signals were visualized in a confocal ultra-espectral microscope TCS-SP5 WLL (Leica). TERC probe was generated from a PCR product by *in vitro* transcription (Ambion AM1312) using Cy3-labelled CTP (Amersham) using the following primers: L-TERC1: CGCTGTTTTTCTCGCTGACT, R-TERC4-T7: ccaagcttctaatacgactcactatagggagaCCCACAGCTCAGGTAAGACA

RNA-FISH in iPS cells was performed basically as described before (Lopez de Silanes et al., 2014) with some modifications: hybridization with the TERC probe described above was performed at 45º C, and washes were done at 48º C. Immunofluorescence was performed with a rabbit polyclonal antibody against TRF1 (raised in our laboratory against full-length mouse TRF1 protein).

Microscopy

Fluorescent images were acquired in a TCS-SP5 (AOBS) laser scanning confocal microscope (Leica mycrosistems) with a 63X HCX PL APO 1.42 N.A. Nuclear staining for TRF1, OCT4, NANOG, H4K20me3, H3K9me3 and telomere analysis was performed with Definiens Developer XD 64 v2.3 image analysis software (Definiens).

Supplemental References

Abad, M., Mosteiro, L., Pantoja, C., Canamero, M., Rayon, T., Ors, I., Grana, O., Megias, D., Dominguez, O., Martinez, D., *et al.* (2013). Reprogramming in vivo produces teratomas and iPS cells with totipotency features. Nature *502*, 340-345.

Blasco, M.A., Lee, H.W., Hande, M.P., Samper, E., Lansdorp, P.M., DePinho, R.A., and Greider, C.W. (1997). Telomere shortening and tumor formation by mouse cells lacking telomerase RNA. Cell *91*, 25-34.

Lopez de Silanes, I., Grana, O., De Bonis, M.L., Dominguez, O., Pisano, D.G., and Blasco, M.A. (2014). Identification of TERRA locus unveils a telomere protection role through association to nearly all chromosomes. Nat Commun *5*, 4723.

Schneider, R.P., Garrobo, I., Foronda, M., Palacios, J.A., Marion, R.M., Flores, I., Ortega, S., and Blasco, M.A. (2013). TRF1 is a stem cell marker and is essential for the generation of induced pluripotent stem cells. Nat Commun *4*, 1946.